

Category Level Pick and Place Using Deep Reinforcement Learning

Marcus Gualtieri, Andreas ten Pas, and Robert Platt

Abstract This paper proposes a new formulation of robotic pick and place. We formulate pick and place as a deep RL problem where the actions are grasp and place poses for the robot’s hand, and the state is encoded with the observed geometry local to a selected grasp. This framework is well-suited to learning pick and place tasks involving novel objects in clutter. We present experiments demonstrating that our method works well on a new variant of pick and place tasks which we call *category level pick and place* where the category of the object to be manipulated is known but its exact appearance and geometry is unknown. The results show, even though these are novel objects and they are presented in clutter, our method can still grasp, re-grasp, and place them in a desired pose with high probability.

1 Introduction

Traditional approaches to robotic manipulation require precise estimates of the pose of all relevant objects [4, 11, 17]. For example, in order to insert a cap onto a bottle, it is common to estimate the pose of the bottle and the cap and then to plan a sequence of manipulation motions that would connect them. However, this approach can run into trouble for at least two reasons. First, the combined configuration space of the two objects (in which planning would occur) is at least twelve dimensional, making planning non-trivial even in this simple scenario. Second, it can be challenging to estimate the pose of the objects to be manipulated with sufficient accuracy to ensure that manipulation is successful. These two challenges are particularly problematic for novel objects presented in open world scenarios.

Approaches based on deep reinforcement learning (deep RL) are an alternative to the model based approach described above [13]. Recent work has shown that deep RL has the potential to alleviate some of the perceptual challenges in manipulation. In

College of Computer and Information Science, Northeastern University
Boston, Massachusetts, USA

particular, Levine et al. showed that deep learning in conjunction with policy gradient reinforcement learning can learn a control policy expressed directly in terms of sensed RGB images [10]. Not only does this eliminate the need to develop a separate perceptual process for estimating state, but it simplifies the perceptual problem by enabling the system to focus only on the perceptual information relevant to the specific manipulation problem to be solved. This, along with encoding actions using low level robot commands (such as motor torque or Cartesian motion commands [9, 10]), means that the approach is quite flexible: a variety of different manipulation behaviors can be learned using exactly the same state/action framework by varying only the reward function.

Unfortunately, there are some drawbacks to this approach as well. The fact that it learns control policies expressed in terms of raw images and low-level motions or torques means it can be hard to learn complex multi-step manipulation behaviors. Moreover, because learning happens at the low level and there is no abstraction from the image produced by a camera, it is difficult to learn policies that generalize to novel objects, novel environments, or even novel camera viewpoints. Finally, it is not clear how to transfer knowledge learned in one task to another. There is no structure in the learned low-level control policies that would facilitate such transfer.

This paper proposes an new method of structuring robotic manipulation as a deep RL problem. Rather than expressing the problem in terms of low-level motor commands and raw images, our formulation encodes the problem at a slightly higher level of abstraction: at the level of grasp and place actions. Each grasp or place action is associated with an image-based descriptor that encodes the destination of a candidate motion relative to a point cloud. We use a variant of deep RL to learn an action value function that approximates the value of each of these motions in terms of the visual descriptors. This approach has a couple of advantages relative to standard deep RL approaches. First, since our action set contains endpoint motions rather than just low level motor commands, we can encode complex manipulation behaviors with longer time horizons (up to 10 actions in our experiments). This enables us to learn faster and to train the system to handle a greater degree of object and environment variability. Second, since our visual descriptors are referenced to surfaces in the environment rather than to the robot frame, our learned feature representations generalize more easily to new situations. We evaluate the approach in the context of a new class of tasks we call *category level pick and place problems* where the robot must move or manipulate objects drawn from a known category but have a novel geometry. For example, the task might be to grasp a bottle and place it upright on a shelf where the exact appearance or geometry of the bottle is unknown in advance (see Figure 1). The fact that we address this class of



Fig. 1 Illustration of the category level pick and place problem considered in this paper. The robot must grasp and place an object in a desired pose without prior knowledge of its shape.

tasks is significant because: 1) it is a practical problem because we may not know the precise geometry of objects to be manipulated in advance and 2) there are no algorithms we know of for picking novel objects and placing them in a desired pose precisely. We show our method is relevant for “simple” pick and place tasks where the robot can solve the task by performing a single grasp and a single place or even more complex pick and place tasks where the robot must re-grasp in order to place the object in a desired pose. We evaluate both in simulation and on a real robot and show significant improvement relative to a baseline where object pose is estimated using shape primitives.

2 Problem Statement

Pick and place problems are relatively well studied in robotics and industry. The basic problem is to pick up an object by grasping it and to place it in a desired configuration. Traditionally, it is assumed the precise geometry and appearance of the object to be picked/placed is known in advance and only a single grasp and place sequence will occur, i.e., the object will be grasped once and placed once. In this work, we relax both of these assumptions. Our goal is to move an object into a desired pose by performing a sequence of one or more pick and place actions. Moreover, we allow that the precise geometry and appearance of the object is unknown. Our only assumption is that the object *category* is known – hence we call our version of the problem “category level pick and place”.

Problem 1 (Category level pick and place). Given a continuous space of possible object geometries O , a reference frame $T(o) \in SE(3)$ associated with each object $o \in O$, a region of interest $\mathcal{R} \subseteq \mathbb{R}^3$, a set of goal poses $g \subseteq SE(3)$, and a model of the robot manipulator and its sensors, calculate a policy for moving any object $o \in O$, from \mathcal{R} to a pose $T(o) \in g$.

The problem statement above is distinguished from the standard pick and place problem by the fact we require the robot to be able to move *any* object, $o \in O$, into the goal pose rather than a specific object with known geometry. Each object is associated with a 6-DOF reference frame, $T(o)$, that together with g , defines the goal configuration for that particular object. The region of interest, \mathcal{R} , is a subset of Cartesian space in which one or more target objects lie. As O becomes smaller, ultimately approaching a single point, Problem 1 reduces to the standard problem. However, when O includes many differently shaped objects, a strategy is needed that generalizes well across objects in O .

3 Approach

3.1 Simulation With Constrained Actions and Percepts

Deep RL requires such an enormous amount of experience that it is difficult to learn control policies on real robotic hardware without spending months or years in training [9, 10]. As a result, learning in simulation is basically a requirement. Unfortunately, simulating the dynamics of arbitrary contacts between a robot and the environment can be challenging because it typically requires solving a linear complementarity problem. Moreover, it can be difficult to simulate sensor data accurately – RGB images in particular are difficult to render realistically. Both of these issues can cause problems: if the contact dynamics are not sufficiently accurate or if the simulated sensor data is not sufficiently realistic, then the policies learned in simulation will fail to translate into real life.

Rather than trying to simulate contact better, our basic approach in this paper is to constrain the space of allowed actions and percepts to things that are easy to simulate. First, we disallow non-prehensile contact between the robot and the environment, i.e., we disallow pushing, throwing, sliding, etc. We only allow grasping and placement motions. This simplifies the simulation problem considerably. If we are only concerned with predicting whether a given contact interaction will result in a grasp, then we can accomplish this just by evaluating a grasp quality metric [14]. Similarly, if we only need to evaluate whether an object will fall over after being placed, we can just identify some sufficient conditions for an object not to fall over, e.g., that it be released less than 1cm above a flat surface with an angle of less than 20 degrees relative to the vertical. Both these conditions are easy to evaluate in OpenRave [2], the kinematic simulator used in this work. Also, we constrain the type of sensor feedback: we only allow point clouds. Unlike RGB images, point clouds are relatively easy to simulate using ray casting. While this approach to simulation certainly reduces the types of policies the robot can learn, it dramatically simplifies the simulation problem and makes it much easier to collect the large amount of experience deep RL requires.

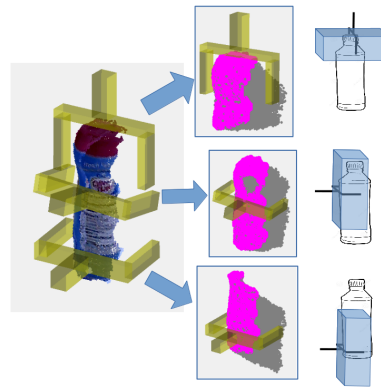


Fig. 2 Examples of the grasp descriptor for the three grasps shown on the left. The right column shows the cuboid associated with each grasp. The middle column shows the descriptor: the visible and occluded points contained within the cuboid.

3.2 Grasp Descriptor

A key element of our state and action representation is derived from the grasp descriptor developed in our prior work [3]. The grasp descriptor encodes the relative pose between a robot hand and an object in terms of the visible and occluded points in the vicinity of a prospective grasp, as seen by a depth sensor. It also encodes the visible aspects of the object shape in the vicinity of the hand. Figure 2 illustrates the idea. The middle column shows the grasp descriptors corresponding to the three grasps of the object shown on the left. Each descriptor encodes the visible points and the corresponding surface normals contained within a 3d cuboid volume (10cm in depth by 10cm in width by 20cm in height) in the vicinity of the robotic hand, as shown in the right column of Figure 2 (normals not shown). The contents of the cuboid are projected onto planes orthogonal to three different viewing directions, voxelized, and then compiled into a single $60 \times 60 \times 12$ image, as described in [3].

3.3 The Reach MDP

We encode the category level pick and place problem (Problem 1) as a Markov Decision Process (MDP) where the actions are collision-free grasp and place actions and the states are encoded using the grasp descriptor. The fact that the actions are entire reach actions rather than incremental torque/velocity commands makes this a higher level encoding than is currently typical in deep RL. Nevertheless, it can still be considered a deep RL approach because we encode the action value function using a deep network. Because all arm motions are encoded as a reach to a desired target pose, we call this encoding the *Reach MDP*. As in all model free reinforcement learning problems, the transition function is assumed to be unknown.

State representation: Figure 3 illustrates the Reach MDP. The set of blue circles on the right labeled “Space of all grasp descriptors” denotes the set of states where an object has been grasped. This is a continuous space of states equal to the set of all possible grasp descriptors. Since the grasp descriptor encodes information about both object shape and the pose of the hand relative to the object, our state representation inherits this information as well. The set of blue circles on the left labeled “Space of object placements” represents the set of states where an object has been placed somewhere

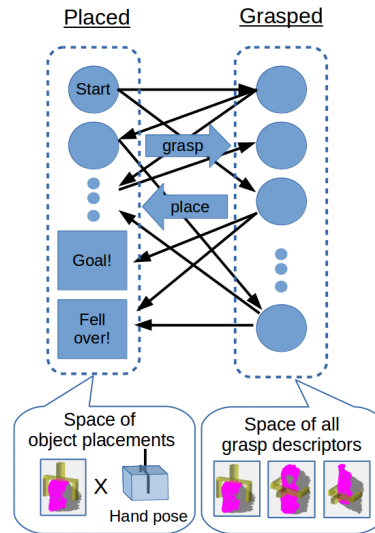


Fig. 3 Reach MDP. States on the right are those where an object is grasped. All other states are on the left.

in the environment. We encode these states in terms of the actions that caused the object to reach that placement. Specifically, it is the cross product between a grasp descriptor and a place action. The grasp descriptor encodes how the object was grasped prior to placement. The place action encodes the pose of the robotic hand at placement. Together, these two pieces of information describe the pose of an object in a scene. The object placement labeled “Goal!” in Figure 3 denotes an absorbing state in the desired final placement pose of the object. The state at the lower left labeled “Fell over!” denotes an absorbing state where the object has been placed incorrectly. When the agent reaches either of these states, it obtains a final reward and the episode ends.

Action representation: There are two types of actions: grasp and place actions. The grasp actions generally result in a transition from a state on the left side of Figure 3 (the space of object placements) to a state on the right side (the space of grasps). The place actions typically result in a transition from right to left. In this work, the place actions are very simple: we require the human designer to specify in advance a set of hand poses that define the set of place actions. Given a particular place action to execute, we plan a collision free motion to the corresponding hand pose and open the fingers. Let PLACE denote the set of place actions. The grasp actions directly leverage our prior grasp pose detection work [3]. Given a point cloud of a scene and a region of interest, our grasp pose detector (GPD) locates a large number of potential grasp configurations. Each detected grasp is a distinct grasp action available for execution. Imagine the set of all possible reach and grip motions that would result in a grasp for a particular scene. We view the process of running GPD as sampling from this set. So, instead of defining the Reach MDP using a fixed set of grasp actions, we are essentially sampling a new set of grasp actions on each time step. Let GRASP_t denote the set of grasp actions sampled at time t . Since we are sampling actions, we need a way to encode the action choice to the action value function, i.e., to the Q-function we encode using a neural network. Our answer is that we encode the action using the corresponding grasp descriptor. So the grasp descriptor is used both to encode the set of potential grasp actions and to encode state, i.e., the results of having executed a particular grasp. The total set of actions available to the agent at time t is $A_t = \text{GRASP}_t \cup \text{PLACE}$.

Reward: Our agent obtains a reward of +1 when it reaches a placement state that satisfies the desired problem constraints, i.e., when it reaches the “Goal!” state in Figure 3. Otherwise, it obtains zero reward.

3.4 The Action Value Function

We approximate the action value function using the convolutional neural network (CNN) shown in Figure 4. The input is an encoding of the state and the action, and the output is a scalar, real value representing the value of that state-action pair. This structure is slightly different than that used in DQN [13] where the network has a number of outputs equal to the number of actions. Here, the fact that our MDP allows

for a large, variable number actions sampled from a continuous space means we must take action as an input to the network. The action component of the input is comprised of the $60 \times 60 \times 12$ grasp descriptor (see Section 3.2) and a one-hot vector denoting the place action selected. When the agent selects a grasp action, the grasp descriptor is populated and the place vector is set to zero. When a place action is selected, the grasp descriptor is set to zero and the place vector populated. The state component of the input is also comprised of a $60 \times 60 \times 12$ grasp descriptor and a place vector. However, the semantics of these two inputs are different from the action input. After executing a grasp action, the grasp descriptor component of state is set to a stored version of the descriptor of the selected grasp and the place vector is set to zero. After executing a place action, the grasp descriptor retains the selected grasp and the place component is set to the just-executed place command, thereby implicitly encoding the resulting pose of the object following the place action. Each grasp image (both in the action input and the state input) is processed by a CNN similar to LeNet [8], except the output has 100 hidden nodes instead of 10. These outputs, together with the place information, are then concatenated and passed into two 60-unit fully connected, inner product (IP) layers, each followed by rectifier linear units (ReLU). After this there is one more inner product to produce the scalar output.

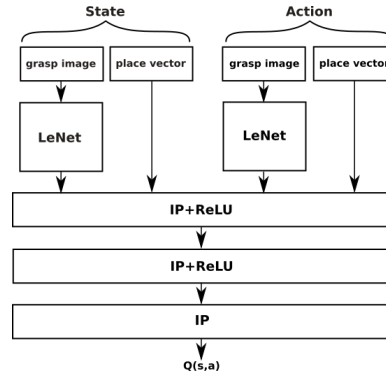


Fig. 4 Convolutional neural network architecture used to encode the action value function, i.e., the Q-function.

3.5 Learning Algorithm

Our learning algorithm is shown in Algorithm 1. This is similar to standard deep Q learning [13], but with a few key differences. First, we use a variant of SARSA [19] rather than Q-learning because the large action branching factor makes the $\max_{a \in A} Q(s, a)$ in Q-learning a bit cumbersome to evaluate. Second, we have an outer **for** loop that iterates over “scenes” and an inner loop that iterates over episodes. This structure enables us to generate $nEpisodes$ of experience for each distinct simulated scene. The problem is that it is significantly more expensive computationally to acquire the depth image and detect grasps than it is to run the rest of the simulation. This structure makes training significantly more efficient. Essentially, we are enabling the agent to explore the many different ways of performing grasp and place actions for each distinct scene. A third difference relative to standard deep Q learning is that we do not run a single stochastic gradient descent (SGD) step after each experience. Instead, we collect $nRounds \times nEpisodes$ of experience before sampling a batch of training data and labeling it using the most recent neural

Algorithm 1: SARSA implementation used in this work

```

1 for  $i \leftarrow 1 : nScenes$  do
2   Randomly choose an object from the training set
3   Place the object in a random configuration with clutter in sim
4   Get a point cloud  $C$  in sim and detect grasps  $G$  in  $C$ 
5    $C_0 \leftarrow C; G_0 \leftarrow G$ 
6   for  $k \leftarrow 1 : nEpisodes$  do
7      $s \leftarrow$  initial state
8     Choose action  $a \in A$  ( $\epsilon$ -greedy)
9     for  $t \leftarrow 1 : T_{max}$  do
10      execute action  $a$ ; observe  $s', r'$ 
11      if  $a \in \text{Place}$  then
12        Get a point cloud  $C$  in sim and detect grasps  $G$  in  $C$ 
13      Choose action  $a' \in A$  ( $\epsilon$ -greedy)
14      Save  $(s, a, r', s', a')$  in database
15      if  $s'$  is terminal then break
16       $s \leftarrow s'; a \leftarrow a'$ 
17    Place object back to its initial, random configuration
18     $C \leftarrow C_0; G \leftarrow G_0$ 
19    if  $\text{mod}(nScenes, nRounds) = 0$  then
20      Prune database if it is larger than  $maxExperiences$ 
21      Label each experience,  $(s, a, r', s', a')$ , as  $Q(s, a) \leftarrow r' + Q(s', a')$ 
22      Run backpropagation for  $nIterations$  with SGD on training batch

```

network weights. Every $nRounds \times nEpisodes$ additional experiences, we create a new randomized batch and run $nIterations$ of SGD using Caffe [6].

4 Experiments in Simulation

We performed experiments in simulation to evaluate how well our approach performs on the category level pick and place problem. To do so, we obtained objects belonging to two different categories for experimentation: a set of 73 bottles and a set of 75 mugs, both in the form of mesh models obtained from 3DNet [22]. Both object sets were partitioned into a 75%/25% train/test split. We performed experiments where our system was trained on the training split and then pick/place success rates were evaluated on the test split.

4.1 Experimental Scenarios

There were three different experimental scenarios, *two-step-isolation*, *two-step-clutter*, and *multi-step-isolation*. In *two-step-isolation*, an object was selected at

random from the training set and placed in a random pose in isolation on a tabletop. The goal condition was a right-side-up placement in a particular position on a table. In this scenario, the agent was only allowed to execute one grasp action followed by one place action (hence the “two-step” label). *Two-step-clutter* was the same as *two-step-isolation* except in this scenario, a set of seven objects was selected at random from the same object category and placed in random poses on a tabletop as if they had been physically “dumped” onto the table.

The *multi-step-isolation* scenario was like *two-step-isolation* except that multiple picks/places were allowed, e.g., the robot could pick up the object, put it down, pick it up again in (potentially) a different way, put it down again, etc., for up to 10 time steps. Also, the goal condition was more restricted: the object needed to be placed right side up inside of a box rather than on a tabletop. Because the target pose was in a box, it became impossible to successfully reach it without grasping the object from the top before performing the final place (see Figure 5). Because the object could not always be grasped in the desired way initially, this additional constraint on the goal state sometimes forced the system to perform a re-grasp in order to achieve the desired pose.

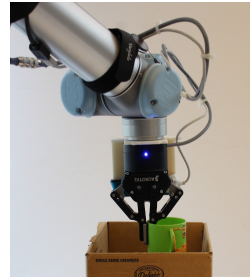


Fig. 5 Goal configuration for multi-step-isolation scenario.

4.2 Algorithm Variations

We compared the performance of two different parameterizations of Algorithm 1 in the two-step-isolation and two-step-clutter scenarios. In the *standard* variation, we used Algorithm 1 with grasp descriptors of the standard size (10cm in depth by 10cm in width by 20cm in height). In the *large-volume* (LV) variation, we used the same algorithm with grasp descriptors evaluated over a larger volume (20cm in depth by 20cm in width by 40cm in height). The algorithm was parameterized as follows. We used 3.5k scenes ($nScenes = 3.5k$ in Algorithm 1). For each scene, we ran 20 episodes ($nEpisodes = 20$). We retrained the CNN by running 5k iterations of SGD once every 50 scenes ($nRounds = 50$) with a batch size of 32. Bottles varied in height between 10 and 20cm. Mugs varied in height between 6 and 12cm. We linearly decreased the exploration factor (epsilon) from 100% down to 10% over the first 18k episodes. In all simulation experiments, we assumed the grasp detector (GPD) was infallible. All point clouds were registered composites of two clouds taken from views above the object and 90° apart.

We compared these two variations with two baselines. The first was the *random baseline*, where grasp and place actions were chosen uniformly at random. The second was the *shape primitives baseline*, where object pose was approximated by segmenting the point cloud and fitting a cylinder. Although it is generally challenging to fit a shape when the precise geometry of the object to be grasped is unknown,

we hypothesized that it could be possible to obtain good pick/place success rates by fitting a cylinder and using simple heuristics to decide which end should be up. We implemented this as follows. First, we segment the scene into k clusters, using k -means ($k = 1$ for isolation and $k = 7$ for clutter). Then we fit a cylinder to the most isolated cluster using MLESAC [20]. We select the grasp most closely aligned with and nearest to the center of the fitted cylinder. The height of the placement action is determined based on the length of the fitted cylinder. The grasp up direction is chosen to be aligned with the cylinder half which contains fewer points. In order to get the shape primitive baseline to work, we had to remove points on the table plane from the point cloud. Although our learning methods do not require this and work nearly as well either way, we removed the table plane in all simulation experiments for consistency.

4.3 Results for the Two-Step Scenarios

Trained With / Tested With	Bottle in Iso.	Bottles in Clut.	Mug in Iso.	Mugs in Clut.
Isolation	1.00	0.67	0.84	0.60
Clutter	0.78	0.87	0.74	0.75
Isolation LV	0.99	0.47	0.91	0.40
Clutter LV	0.96	0.80	0.67	0.70
Shape Primitives Baseline	0.43	0.24	0.08	0.12
Random Baseline	0.02	0.02	0.02	0.02

Table 1 Average correct placements over 300 episodes for bottles after training (i.e., fixed network weights and $\epsilon = 0$). *LV* is the *large-volume* variation, *shape primitives baseline* is with fitting cylinders, and *random baseline* is with random grasp and place actions.

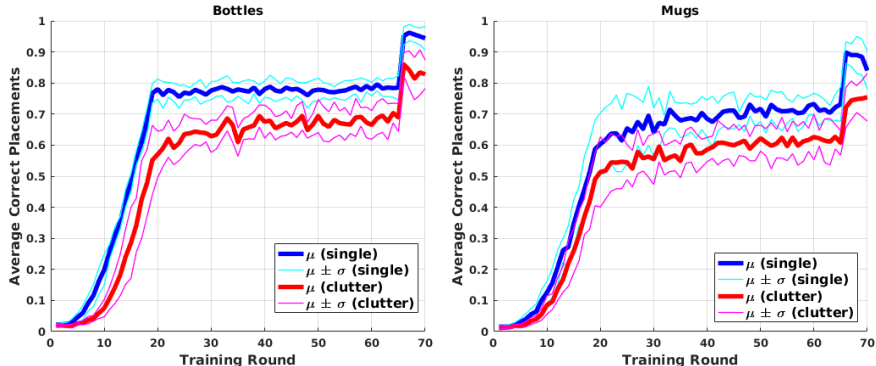


Fig. 6 Average of 10 learning curves for the two-step scenario. The “training round” on the horizontal axis denotes the number of times Caffe had been called for a round of 5k SGD iterations. The left plot is for bottles and the right for mugs. Blue denotes single objects and red denotes clutter. Curves for mean plus and minus standard deviation are shown in lighter colors. The sharp increase in performance during the last five rounds in each graph is caused by dropping the exploration factor (ϵ) from 10% to 0% during these rounds.

We trained our algorithm in four different scenarios: bottles in isolation, bottles in clutter, mugs in isolation, and mugs in clutter. Figure 6 shows learning curves for four contingencies averaged over 10 runs. Table 1 shows pick/place success rates for various algorithm variations in various scenarios averaged over 300 trials. A pick/place episode was only considered to be successful if the object was placed within 3cm of the table and 20 degrees of the vertical in the desired pose. The rows correspond to different algorithm variations trained with and without clutter. For example, the first row shows performance when training using only objects presented in isolation using the *standard* variation of Algorithm 1. The columns correspond to various different test scenarios. For example, the “Bottles in Clut.” column is where the system was evaluated with 7 bottles dropped on the table, even if training was done with isolated objects.

Several results are worth highlighting. First, notice our algorithm does very well with respect to the baselines. The random baseline (last row) succeeds only 2% of the time – suggesting that the problem is indeed challenging. The shape primitives baseline (where we localize objects by fitting cylinders) also does relatively poorly: it succeeds at most only 43% of the time for bottles and only 12% of the time for mugs. Second, notice the variation in the performance of our algorithm under various conditions and scenarios. Pick/place success rates are lower when objects are presented in clutter compared to isolation: 100% success versus 87% success rates for bottles; 84% versus 75% success for mugs. Also, if evaluation is to be in clutter (resp. isolation), then it helps to train in clutter (resp. isolation) as well: if trained only in isolation, then clutter success rates for bottles drops from 87% to 67%; clutter success rates for mugs drops from 75% to 60%. Also, notice that using the larger grasp descriptor (LV) can improve grasp success rates in isolation (an increase of 84% to 91% for mugs), but hurts when evaluated in clutter: a decrease from 87% to 80% for bottles; a decrease from 75% to 70% for mugs. We suspect that this drop in performance reflects the fact that in clutter, the large receptive field of the LV descriptor encompasses “distracting” information created by other objects nearby the target object (remember that we do not use segmentation) [12].

4.4 Results for the Multi-Step Scenario

Training for the multi-step-isolation scenario is the same as it was in the two-step scenario except we doubled the number of episodes ($nScenes = 7.5k$ instead of $nScenes = 3.5k$) because the longer policies took longer to learn. Recall that this scenario involved a time horizon of up to 10 time steps where the robot needed to place the mug inside of a box by grasping it from the top. We only performed this experiment using mugs (not bottles) because it was difficult for our system to grasp many of the bottles in our dataset from the top. Figure 7 shows the number of successful non-goal and goal placements as a function of training round.¹ Initially,

¹ Non-goal placements were considered successful if the object was 3cm or less above the table. Any orientation was allowed. Unsuccessful non-goal placements terminate the episode.

the system does not make much use of its ability to perform intermediate placements in order to achieve the desired goal placement, i.e., to pick up the mug, put it down, and then pick it up a second time in a different way. This is evidenced by the low values for non-goal placements (the blue line) prior to round 60. However, after round 60, the system learns the value of the non-goal placement, thereby enabling it to increase its final placement success rate to its maximum value (around 90%). Essentially, the agent learns to perform a non-goal placement when the mug cannot immediately be grasped from the top or if the orientation of the mug cannot be determined from the sensor perception. After learning is complete, we obtain an 84% pick and place success rate averaged over 300 test set trials.

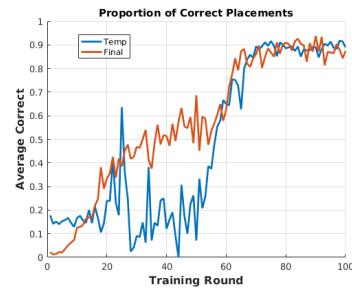


Fig. 7 Red line: number of successful pick/place trials as a function of training round (number of times we run 5k iterations of SGD in Caffe). Blue line: number of successful non-goal placements executed.

5 Experiments on a Real Robot

We evaluated the same three scenarios on the real robot that we did in simulation: *two-step-isolation*, *two-step-clutter*, and *multi-step-isolation*. As before, the two step scenarios were evaluated for both bottles and mugs and the multi-step scenario was evaluated for only mugs. The experiments were performed by a UR5 robot, equipped with a Robotiq parallel-jaw gripper and a wrist-mounted Structure depth sensor (see Figure 9). Two sensor views were always taken from fixed poses, 90° apart. The object set included 7 bottles and 6 mugs, as shown in Figure 8. We used only objects that fit into the gripper, would not shatter when dropped, and had a non-reflective surface visible to our depth sensor. Some of the lighter bottles were partially filled so small disturbances (e.g., sticking to fingers) would not cause a failure. Figure 9 shows several examples of our two-step scenario for bottles presented in clutter.

In order to get reasonable pick/place success rates on the real robot, we found that we needed to adjust the algorithm and its parameters in a few minor ways. First, we changed the conditions for a successful place used by the simulator during training. In our simulation experiments, a successful place was deemed to have occurred when the bottom of the object was placed less than 3cm above the table and the orientation was within 20 degrees of the vertical. However, during our initial experiments, we found that our policy sometimes selected placements



Fig. 8 The seven novel bottles and six novel mugs used to evaluate our approach in the robot experiments.

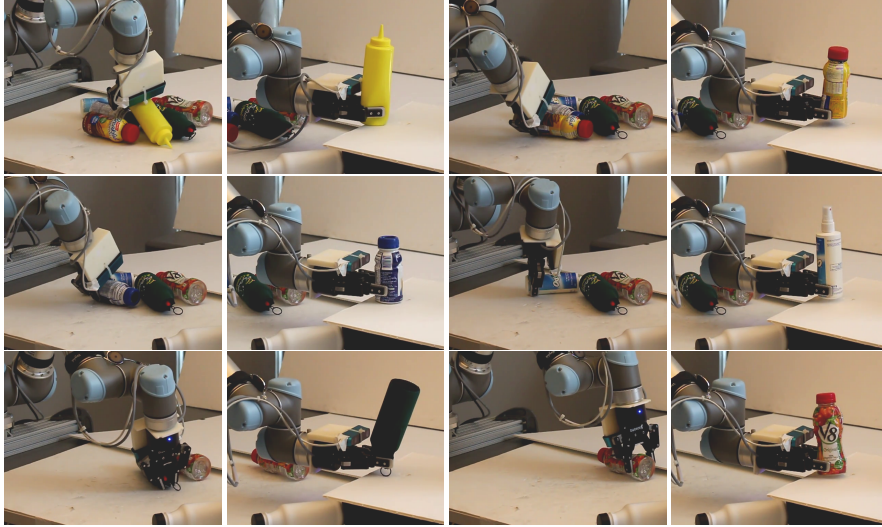


Fig. 9 Examples of the two-step clutter scenario for bottles. Notice the failure in the two lower left images.

that caused the objects to fall over. As a result, we adjusted the maximum place height during simulation from 3cm to 2cm and changed the reward function to fall off exponentially for altitudes higher than 2 cm. We also raised the acceptance threshold used by our grasp detector (GPD [3])² and removed table plane filtering (remember that we filtered points in the table plane during training in order to facilitate our shape primitive baseline). Finally, we created a mechanism for the policy to “declare failure” and re-start a run prior to the first grasp. If the initial probability of success was found to be less than 20% prior to the first grasp, i.e., the maximum action value of the initial state was less than 0.2, then our system immediately re-started the episode by acquiring a new point cloud and rerunning GPD.

	1 Bottle	7 Bottles	1 Mug	6 Mugs	Re-grasp
Grasp	0.96	0.97	0.88	0.80	0.97
Final Place	0.89	0.76	0.80	0.61	0.76
Temporary Place	-	-	-	-	0.77
Entire Task	0.84	0.73	0.70	0.48	0.55
Number of Trials	112	97	96	91	72
Upside-down	5	19	5	4	0
Sideways	0	0	7	18	9
Fell Over	2	3	1	2	0

Table 2 (Top) Success rates for grasp, temporary place, final place, and entire task. (Bottom) Placement error counts by type. Results are averaged over the number of trials shown in the middle.

² GPD outputs a machine-learned probability of a stable (i.e., force closure) grasp. The *threshold* is the grasp stability probability above which grasps are accepted.

Table 2 summarizes the results from our robot experiments. We performed 468 pick and place trials over five different scenarios. Column 1 of Table 2 shows results for pick and place for a single bottle presented in isolation averaged over all bottles in the seven-bottle set. Out of 112 trials, 96% of the grasps were successful and 89% of the placements were successful, resulting in a complete task pick/place success rate of 84%. Column 2 shows similar results for the bottles-in-clutter scenario, and columns 3 and 4 include results for the same experiments with mugs. Finally, column five summarizes results from the multi-step-isolation scenario for mugs: overall, our method succeeded in placing the mug into the box 55% of the time.

6 Discussion

As far as we know, we are the first to identify and define category level pick and place as an interesting problem. The problem is challenging because it is hard to imagine how a planning-based method might reason about manipulating an object that cannot be localized and has no explicitly defined object reference frame. We propose an approach based on deep RL that we show can achieve “reasonable” success rates (our pick/place success rates range from 84% to 48%, see Section 5). This is significant for at least two reasons. First, we are the first to define and address the problem. While performance could certainly be improved, our work demonstrates the method has potential to perform well. Second, we show that deep RL can be applied to robotics at a higher level of abstraction than is currently typical. Currently, most applications of deep RL to robotics learn relatively low level controllers. In this work, we show that a variant of deep RL could be used to learn relatively complex re-grasping behavior that would typically be considered to require geometric planning.

Our experimental results are interesting for several reasons beyond just demonstrating that the method can work. First, we noticed consistently lower pick/place performance for the mug category relative to the bottle category. The reason for this is that there is more perceptual ambiguity involved in determining the orientation of a mug compared to that of a bottle. In order to decide which end of a mug is “up”, it is necessary for the sensor to view “into” at least one end of the mug. However, since our scenarios placed the mugs in random initial configurations, our predetermined viewing directions sometimes did not view the mugs from the correct perspectives, thereby causing additional place failures. One way to address this problem in the future might be to develop a strategy for intelligently selecting viewpoints, given task context.

Another unexpected experimental result was that our learned policies typically prefer particular types of grasps, e.g., to grasp bottles near the bottom (see Figure 9). We suspect that this is a result of the link between the location of a selected grasp and the grasp descriptor used to represent state. In order to increase the likelihood that the agent will make high-reward decisions in the future, it selects a grasp descriptor that enables it to easily determine the pose of the object. In the case of bottles, descriptors near the base of the bottle best enable it to determine which end is “up”.

Known limitations to our approach include the assumption in simulation that grasps always succeed (which could be addressed with higher fidelity, more time-consuming simulation), inability to recognize correct objects when the clutter contains objects from multiple classes (which could be addressed by augmenting an object detector), and fixed place options (which we plan to address in future work).

7 Related Work

The traditional approach to robotic pick and place is to first estimate the object’s pose and then to plan motions that re-orient the object to a desired, target pose. For example Nguyen *et al.* estimate the object’s pose, grasp a part of the object known to be graspable, and then reorient and place the object [17]. This procedure can repeat multiple times until the object reaches the target pose. Lin *et al.* focus on the perception part of the pick and place problem where objects are presented in light clutter [11]. They also view determining the object’s pose as the necessary first step. Harada *et al.* use a cylinder fitting method to estimate the object’s pose to pick from a dense pile of bananas [4]. Their cylinder fitting mechanism is admittedly more sophisticated than our shape primitives baseline as they use a probabilistic model to adjust the cylinder size and to rank the grasps. However, all of the work described above either only works on the exact object used in training or only generalizes to objects very similar in appearance. Pose estimation for novel objects in a given category is an active area of research [5, 18, 21].

On the other hand, Jiang *et al.* show how to place new objects in new place areas without explicitly estimating the object’s pose [7]. Their placements are sampled instead of, as in our case, fixed. However they do not jointly reason about the grasp and the place – the grasp is predefined. Also their learning method relies on segmenting the object, segmenting the place area, hand-picked features, and human annotation for place appropriateness.

The idea of assigning task semantics to grasps is related to the pick and place problem. Dang and Allen introduced the term “semantic grasp” and showed how to learn semantic grasps given object category [1]. Myers *et al.* and Nguyen *et al.* more recently proposed methods for detecting object affordances [15, 16]. With these methods, the robot learns semantic grasps in a supervised fashion, whereas with our approach the robot learns from trial-and-error and a reward signal. Also, these papers are focused on detecting the task-relevant object parts and/or grasps whereas ours is focused on performing the task itself.

References

1. Dang, H., Allen, P.: Semantic grasping: Planning robotic grasps functionally suitable for an object manipulation task. In: IEEE/RSJ Int’l Conf. on Intelligent Robots and Systems, pp.

- 1311–1317 (2012)
2. Diankov, R.: Automated construction of robotic manipulation programs. Ph.D. thesis, Robotics Institute, Carnegie Mellon University (2010)
 3. Gualtieri, M., ten Pas, A., Saenko, K., Platt, R.: High precision grasp pose detection in dense clutter. In: IEEE Int'l Conf. on Intelligent Robots and Systems (2016)
 4. Harada, K., Nagata, K., Tsuji, T., Yamanobe, N., Nakamura, A., Kawai, Y.: Probabilistic approach for object bin picking approximated by cylinders. In: IEEE Int'l Conf. on Robotics and Automation, pp. 3742–3747 (2013)
 5. Hinterstoisser, S., Cagniard, C., Ilic, S., Sturm, P., Navab, N., Fua, P., Lepetit, V.: Gradient response maps for real-time detection of textureless objects. IEEE Trans. on Pattern Analysis and Machine Intelligence **34**(5), 876–888 (2012)
 6. Jia, Y., Shelhamer, E., Donahue, J., Karayev, S., Long, J., Girshick, R., Guadarrama, S., Darrell, T.: Caffe: Convolutional architecture for fast feature embedding. In: ACM Int'l Conf. on Multimedia, pp. 675–678 (2014)
 7. Jiang, Y., Zheng, C., Lim, M., Saxena, A.: Learning to place new objects. In: Int'l Conf. on Robotics and Automation, pp. 3088–3095 (2012)
 8. LeCun, Y., Bottou, L., Bengio, Y., Haffner, P.: Gradient-based learning applied to document recognition. Proc. of the IEEE **86**(11), 2278–2324 (1998)
 9. Levine, S., Finn, C., Darrell, T., Abbeel, P.: End-to-end training of deep visuomotor policies. Journal of Machine Learning Research **17**(1), 1334–1373 (2016)
 10. Levine, S., Pastor, P., Krizhevsky, A., Quillen, D.: Learning hand-eye coordination for robotic grasping with large-scale data collection. In: Int'l Symposium on Experimental Robotics, pp. 173–184. Springer (2016)
 11. Lin, H.I., Chen, Y.Y., Chen, Y.Y.: Robot vision to recognize both object and rotation for robot pick-and-place operation. In: Int'l Conf. on Advanced Robotics and Intelligent Systems, pp. 1–6. IEEE (2015)
 12. Mnih, V., Heess, N., Graves, A., Kavukcuoglu, K.: Recurrent models of visual attention. In: Advances in neural information processing systems, pp. 2204–2212 (2014)
 13. Mnih, V., Kavukcuoglu, K., Silver, D., Rusu, A., Veness, J., Bellemare, M., Graves, A., Riedmiller, M., Fidjeland, A., Ostrovski, G., Petersen, S., Beattie, C., Sadik, A., Antonoglou, I., King, H., Kumaran, D., Wierstra, D., Legg, S., Hassabis, D.: Human-level control through deep reinforcement learning. Nature **518**(7540), 529–533 (2015)
 14. Murray, R., Li, Z., Sastry, S.: A mathematical introduction to robotic manipulation. CRC press (1994)
 15. Myers, A., Teo, C., Fermüller, C., Aloimonos, Y.: Affordance detection of tool parts from geometric features. In: IEEE Int'l Conf. on Robotics and Automation, pp. 1374–1381 (2015)
 16. Nguyen, A., Kanoulas, D., Caldwell, D., Tsagarakis, N.: Detecting object affordances with convolutional neural networks. In: IEEE/RSJ Int'l Conf. on Intelligent Robots and Systems, pp. 2765–2770 (2016)
 17. Nguyen, A., Kanoulas, D., Caldwell, D., Tsagarakis, N.: Preparatory object reorientation for task-oriented grasping. In: IEEE/RSJ Int'l Conf. on Intelligent Robots and Systems, pp. 893–899 (2016)
 18. Pauwels, K., Kragic, D.: Simtrack: A simulation-based framework for scalable real-time object pose detection and tracking. In: IEEE/RSJ Int'l Conf. on Intelligent Robots and Systems, pp. 1300–1307 (2015)
 19. Rummery, G.A., Niranjan, M.: On-line Q-learning using connectionist systems. CUED/F-INFENG/TR 166, Cambridge University Engineering Department (1994)
 20. Torr, P., Zisserman, A.: Mlesac: A new robust estimator with application to estimating image geometry. Computer Vision and Image Understanding **78**(1), 138–156 (2000)
 21. Wohlhart, P., Lepetit, V.: Learning descriptors for object recognition and 3d pose estimation. In: Proc. of the IEEE Conf. on Computer Vision and Pattern Recognition, pp. 3109–3118 (2015)
 22. Wohlkinger, W., Aldoma, A., Rusu, R., Vincze, M.: 3dnet: Large-scale object class recognition from cad models. In: IEEE Int'l Conf. on Robotics and Automation, pp. 5384–5391 (2012)